Accepted Manuscript

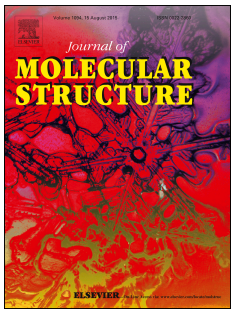

Synthesis, crystal structure, DFT calculations, Hirshfeld surfaces, and antibacterial activities of schiff base based on imidazole

Siham Slassi, Mohammed Aarjane, Khalid Yamni, Amina Amine

PII: S0022-2860(19)30915-9

DOI: https://doi.org/10.1016/j.molstruc.2019.07.071

Reference: MOLSTR 26824

To appear in: *Journal of Molecular Structure*

Received Date: 3 March 2019

Revised Date: 1 July 2019

Accepted Date: 16 July 2019

Please cite this article as: S. Slassi, M. Aarjane, K. Yamni, A. Amine, Synthesis, crystal structure, DFT calculations, Hirshfeld surfaces, and antibacterial activities of schiff base based on imidazole, *Journal of Molecular Structure* (2019), doi: https://doi.org/10.1016/j.molstruc.2019.07.071.

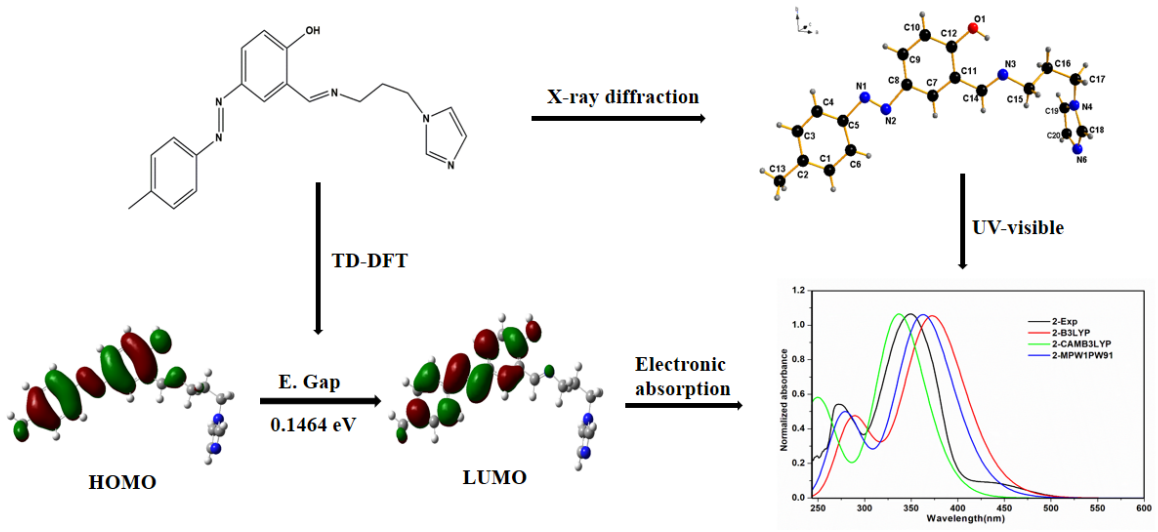

Synthesis, Crystal structure, DFT calculations, Hirshfeld surfaces, and Antibacterial activities of Schiff base based on imidazole

Siham Slassi[a], Mohammed Aarjane[a], Khalid Yamni[b], Amina Amine[a*]

[a] *LCBAE, Equipe Chimie Moléculaire et Molécules Bioactives, Faculté des Sciences Université Moulay Ismail*, BP 11201 Zitoune, *Meknès, Morocco.*
** Corresponding author: amine_7a@yahoo.fr*

[b] *Laboratoire de Chimie des Matériaux et Biotechnologie des Produits Naturels, E.Ma.Me.P.S., Université Moulay Ismail, Faculté des Sciences, Meknès, Morocco.*

Abstract:

A new Schiff base **2** was synthesized by condensation of 2-Hydroxy-5-(p-tolyldiazenyl)benzaldehyde and N(-3-aminopropyl)imidazole, and characterized by IR, ^{1}H NMR, ^{13}C NMR, mass spectroscopy and elemental analysis. Crystal structure of 2 has been determined by X-ray diffraction analysis. The structural parameters and electronic absorption properties of **2** were also studied using Density Functional Theory (DFT), and Time Dependant Density Functional Theory (TD-DFT). Computations were performed at DFT/B3LYP/6-31G(d), DFT/CAMB3LYP/6-31G(d) and DFT/MPW1PW91/6-31G(d) levels of theory. The calculation results of the structural parameters and electronic absorption properties for compound **2** are presented and compared with the X-ray analysis result and UV-visible spectrum. Hirshfeld surface analysis was used to show surface contours and two-dimensional fingerprint plots have been used to analyse intermolecular interactions. The schiff base **2** was assessed for its in vitro antibacterial activities against four pathogenic strains: *Staphylococcus aureus*, *Pseudomonas putida*, *Klebsiella pneumoniae* and *Escherichia coli*.

Keywords: Schiff base, X-ray diffraction, DFT, Electronic absorption, Hirshfeld surfaces, Antibacterial activity.

1. Introduction:

Schiff base compounds have been recognized as privileged among organic molecules, owing to their interesting and important properties. These molecules constitute an important centre of attraction in many areas like biological, clinical, medicinal, analytical and pharmacological fields [1]. They are also used in analytical medicinal and polymer chemistry. The azomethine (C=N) linkage in Schiff bases is significant in determining the mechanism of transamination and resamination reactions in biological systems [2], and it has been suggested that the azomethine group is responsible of the biological activities of Schiff bases molecules. In effect, these molecules are well-known as antibacterial [3,4], antifungal [5,6], anti-inflammatory [7,8], antitumor [9,10], antiviral [11], antipyretic [12], anti-HIV-1 [13] and antiproliferative [14,15]. Furthermore, the azomethine group is an important site for coordinating and stabilizing various metals.

Imidazoles, being the core fragment of different natural products and biological or chemical systems, constitute an important class of heterocycles. The vast therapeutic properties of the imidazole derivatives drugs have encouraged the researchers in the medicinal field to synthesize a huge number of novel molecules based on the imidazole unit as antifungal [6], antibacterial [14,15], antiviral[16,17], anti-inflammatory [18], anticancer [19,20] and antidiabetic agents [21].

In the light of the interesting chemistry of Schiff bases, we herein report the synthesis, characterization and X-ray diffraction of schiff base (**2)** based on imidazole, obtained by condensation of 2-Hydroxy-5-(p-tolyldiazenyl)benzaldehyde and N(3-aminopropyl)imidazole. Using DFT, lowest unoccupied molecular orbital (LUMO) and highest occupied molecular orbital (HOMO) energy levels of frontier orbital were determined. UV-visible spectra were investigated experimentally and theoretically. In addition, Hirshfeld surface analysis was used to analyse intermolecular interactions. The antibacterial activity of **(2)** was evaluated against four pathogenic strains: *Staphylococcus aureus*, *Pseudomonas putida, Klebsiella pneumoniae* and *Escherichia coli*.

2. Results and discussion:

The Schiff base ligand 2 was prepared in excellent yield via the condensation of 2-Hydroxy-5-(o-tolyldiazenyl)benzaldehyde and N-(3-aminopropyl)imidazole then characterized by IR, ^{1}H NMR, ^{13}C NMR, mass spectroscopy, elemental analysis and X-ray diffraction. NMR spectra are reported in Fig. 1and Fig. 2.

2.1 Description of the crystal structure:

The synthesized Schiff base with the general formula ($C_{20}H_{21}N_5O$) crystallizes in the monoclinic space group P2/n. (Table 1) The dihedral angles between the imidazole ring, and the methylphenyl and the phenol groups are 84.39 (16)° and 81.44 (14)° respectively. An intramolecular O–H···N

hydrogen bond forms between the –OH substituent of the phenol ring and the adjacent iminomethyl N atom, enclosing an S6 ring. All the bond lengths are within normal ranges. The N1–N2 and N3–C14 bond lengths, 1.174 (4) and 1.272(4)Å respectively, confirm their double-bond character whereas the N4–C18 and N4—C19 values are 1.347(3) and 1.370(3)Å, respectively.

The asymmetric unit of Schiff base is reported in Fig. 3.

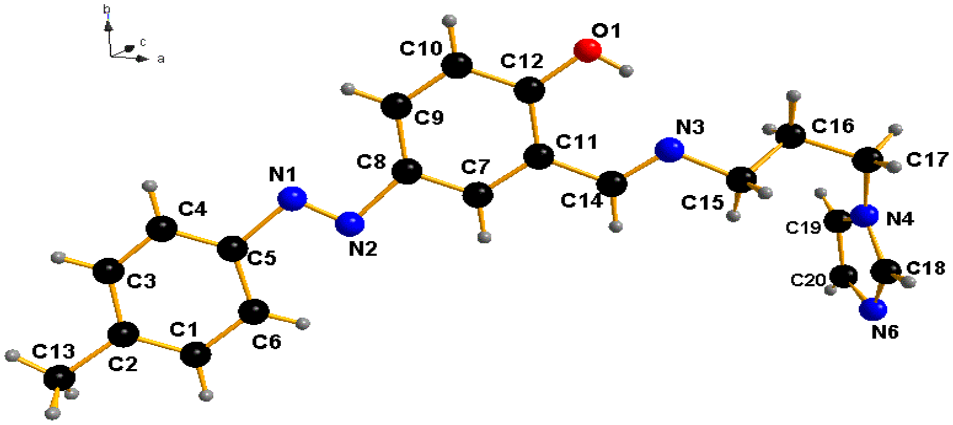

Figure 3: Building unit of the crystal structure of **2**

2.2 Computational Study:

Density functional theory (DFT) computation and time-dependent (TD-DFT) calculations were performed. The structure of **2** was optimized at the B3LYP/6-31G(d) level. As can be observed in Tables 2 and 3, the calculated bond distances and angles are in good agreement with the values obtained from X-ray crystal structure determination. A superposition of the X-ray diffraction and optimized structures of compound **2** is shown in Fig. 4. The negligible differences between the experimental and calculated bond lengths and angles are due to the fact that the computations were performed and calculated in the gas phase, while the X-ray data were obtained in the solid phase.

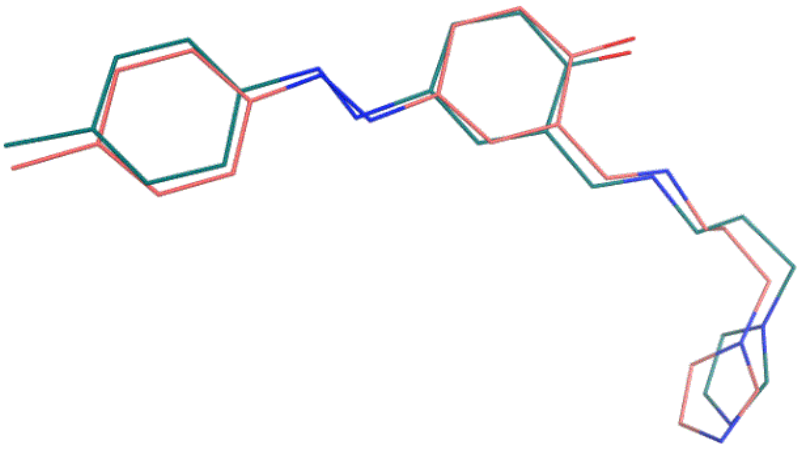

Figure 4: Superposition of X-Ray and optimized structures of **2**.

2.3 Theoretical and experimental UV-visible Spectra study:

UV-vis absorption spectrum of **2** was simulated at TD-DFT/B3LYP/6-31G(d), TD-DFT/CAMB3LYP/6-31G(d) and TD-DFT/MPW1PW91/6-31G(d) levels. The compound was investigated in chloroform by theoretical calculation. Table 4 shows the calculated oscillator strengths (f) and wavelengths (λ) (main transitions) along with the experimental wavelengths. The experimental and theoretical spectra of the compound **2** in chloroform are shown in Fig.5. The obtained results were closer to the experimental absorption wavelengths. We can say that, MPW1PW91 computations lead to a better agreement with experiment relatively to B3LYP and CAMB3LYP. As Fig. 5 exhibits, experimental spectrum of **2** shows three bands at 273, 349 and 437 nm. From the TD–DFT calculation, the most significant theoretical absorption bands of MPW1PW91 were predicted at 279.57, 362.78 nm in chloroform solution.

Table 4: Theoretical and experimental electronic absorption spectral values of **2**

Compound	Excitation level	λ_{max} (nm)	(f)	Electronic transition	Major % Contribution
2	B3LYP	372.85	1.0372	HOMO→LUMO	99.5
		288.67	0.4422	HOMO→LUMO+1	58.6
	CAMB3LYP	336.20	1.0876	HOMO→LUMO	95.8
		254.25	0.4336	HOMO-3→LUMO	69.7
	MPW1PW91	362.78	1.0727	HOMO→LUMO	99.3
		279.57	0.4570	HOMO→LUMO+1	50.5
	Exp	349			
		273			

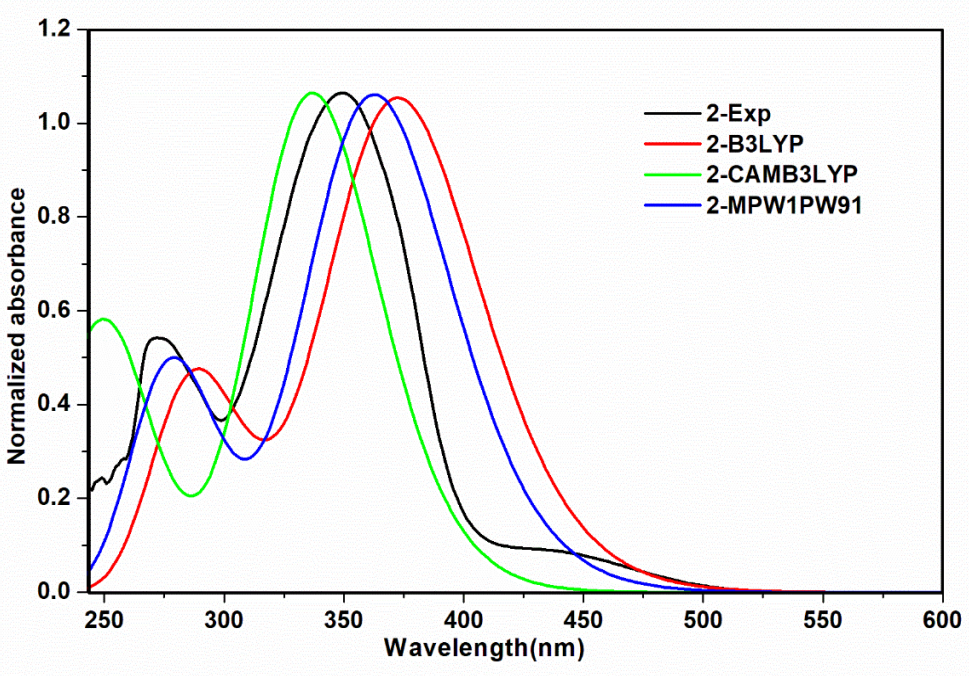

Figure 5: Experimental and theoretical absorption spectra of Schiff base **2** at B3LYP/6-31G (d), CAM-B3LYP/6-31G (d) and MPW1PW91/6-31G(d) levels in $CHCl_3$.

2.4 Frontier Molecular Orbitals (FMOs):

The resulting frontier molecular orbitals for azo-schiff base molecule are reported in Fig.6. The highest occupied molecular orbital HOMO (π donor) is delocalized over the azobenzene moiety including hydroxyl and methyl substituents and azomethine group, the lowest lying unoccupied molecular orbital LUMO (π acceptor) is spread over the azobenzene moiety including only the hydroxyl group. The 279.57 nm transition consists of HOMO → LUMO+1. The 362.78 nm excitation has mainly HOMO → LUMO character.

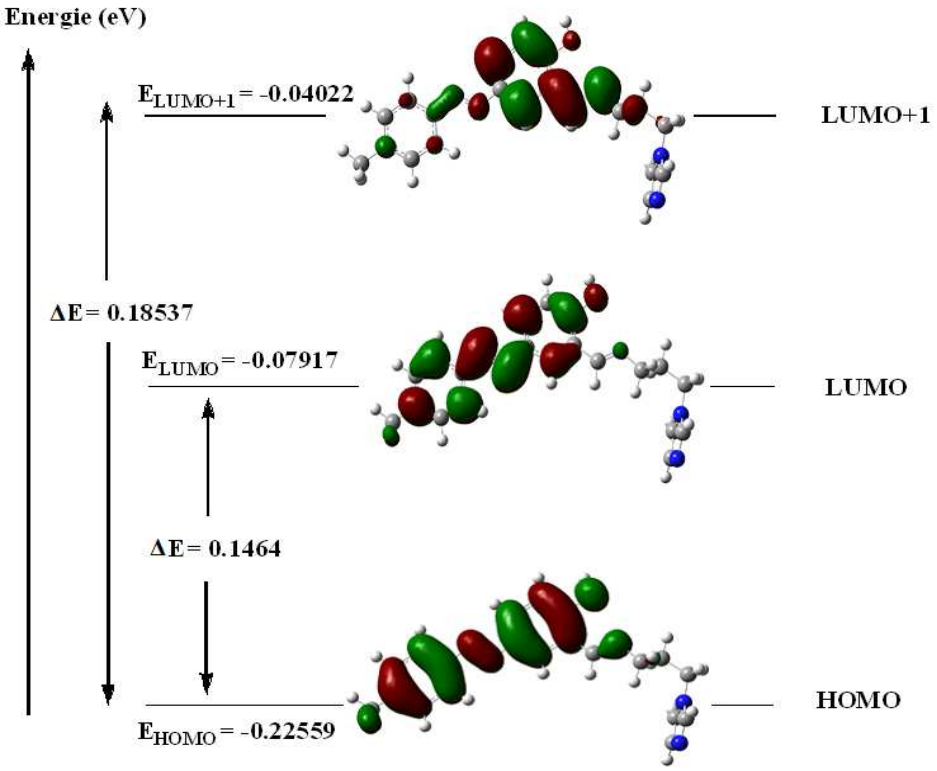

Figure 6: Energy levels and electronic isosurfaces of frontier molecular orbitals.

2.5 Hirshfeld surfaces analysis:

Fig. 7 shows the Hirshfeld surface of the title compound mapped over dnorm (-0.60 to 0.90 A°) and the shape-index (-1.0 to 1.0 A°). In the dnorm map, the vivid red spots in the Hirshfeld surface are due to short normalized O—H distances corresponding to O— H···N interactions. Hydrogen-donor groups constitute the convex blue regions on the shape-index surface and hydrogen-acceptor groups appear in concave red regions. The two dimensional fingerprint plots quantify the contributions of each type of non-covalent interaction to the Hirshfeld surface. The major contribution with 48.6% of the surface is due to H···H contacts, which represent van der waals interactions, followed by C···H, N···H and O···H interactions, which contribute 28.5,15.2 and 6.1%, respectively, these contributions are observed as two sharp peaks in the plot of Fig.8.

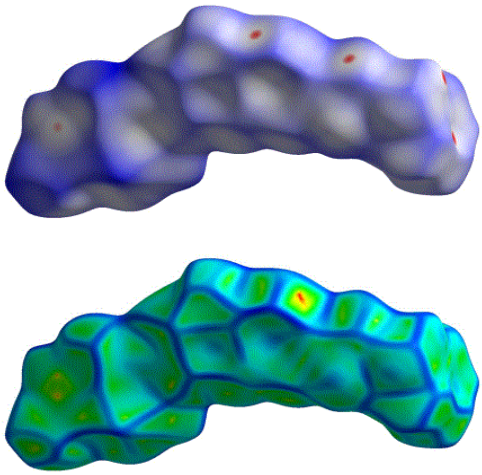

Figure 7: Hirshfeld surfaces for compound (2), mapped with dnorm (top) and shape index (bottom).

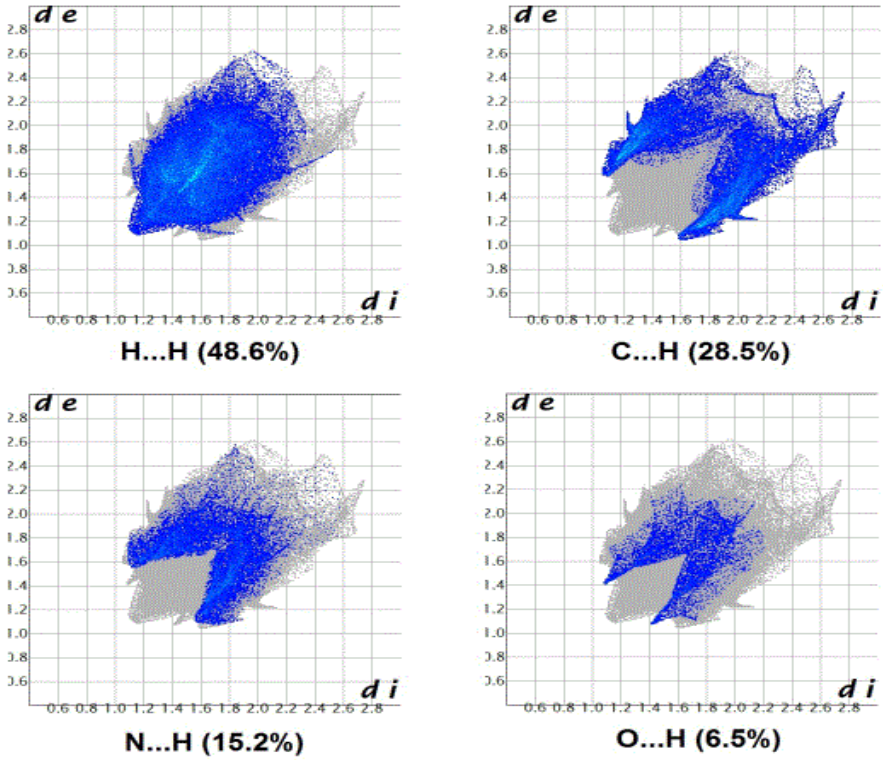

Figure 8: Two-dimensional fingerprints of compound (**2**), showing H···H, C···H, N···H and O···H close contacts.

Voids in the crystal structure of (**2**) (Fig. 9) are built on the sum of spherical atomic electron densities at the appropriate nuclear positions (procrystal electron density). The crystal voids calculation (results under 0.002 a.u. isovalue) shows the void volume of title compound to be of the order of 226.81 $Å^3$ and surface area in the order of 720.59 $Å^2$. The porosity of the calculated void volume of (**2**) is

12.37%. There are no large cavities. We note that the electron-density iso surfaces are not completely closed around the components, but are open at those locations where interspecies approaches are found.

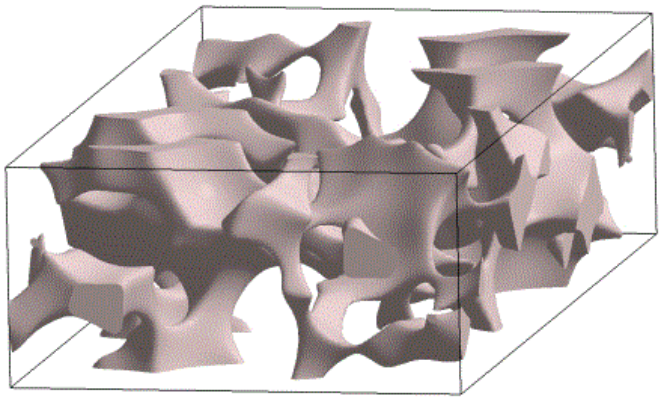

Figure 9: Void plot for (**2**).

2.6 Antibacterial activity:

Firstly, the diffusion agar technique was used to evaluate the antibacterial activity of the Schiff base 2. Schiff base 2 shows the high zone inhibition diameter against *Staphylococcus aureus* 20 mm, then *K. pneumoniae* with 15mm. For *E.coli*, the inhibition zone diameter was 13mm and the lower diameter was observed against *P.putida* with 9mm.

The Minimum inhibitory concentrations (MIC) results of **2** and the commercially available standard are presented in table 5, they agree with those of the disc diffusion test. MICs of the Schiff base **2** against the microorganism species were ranged from 28.84 to 92.10 µg.mL^{-1}. The excellent MIC value was exhibited by **2** against *staphylococcus aureus* (28.84 µg.mL^{-1}). *E.coli* (68.18 µg.mL^{-1}) and *K. pneumoniae* (42.45µg.mL^{-1}) seem to be less sensible to compound **2**. The lower activity was showed against *P.putida* with an MIC value of 92.10 µg.mL^{-1}. The obtained antibacterial activities results of 2 are significant comparing with the activity of the commercialised antibiotic chloramphenicol. In another hand, compound 2 exhibited encouraging antibacterial activities comparing to other reported Schiff bases [22-26]. For instance, the imidazole Schiff base ligand prepared from 1-(3-aminopropyl)imidazole and salicylaldehyde and which was reported first by M. Kalanithi et al. [27] then by J. McGinley et al. [28]. The authors had found the free ligand and its Cu(II) and Zn(II) complexes inactive against a number of tested microbes. Interestingly, for our compound, the functionalization of the salicylate phenyl unit leads to promising antibacterial activities against the selected pathogenic strains indicating the importance of the azo group in the structure of compound 2. Hence, Shiff base **2** could be considered as a potent antibacterial compound.

Table 5: Antibacterial activities determined in liquid medium of 2 (MIC in µg.mL^{-1})

Produit	Bacteria			
	S.aureus	***E.Coli***	***K. pneumoniae***	***P. putida***
2	28.84	68.18	42.45	92.10
Chloramphenicol	11.65	22.41	15.38	37.03
DMSO	-	-	-	-

3. Conclusion:

In sum, the Schiff base ligand **2** has been synthesized and characterized. The crystal structure of the compound was determined by X-Ray diffraction. The geometry and structural parameters of the title compound 2 was optimized with DFT/B3LYP methods using 6-31G(d) basis set. The electronic absorption properties of the compound have been studied using TD-DFT computations at DFT/B3LYP/6-31G(d), DFT/CAMB3LYP/6-31G(d) and DFT/MPW1PW91/6-31G(d) level of theory, analysed and the theoretical results were similar to the experimental ones. Hirshfeld surface analysis gave 2D fingerprint plots showing the intermolecular interactions. The Schiff base **2** was assessed for its in vitro antibacterial activities against pathogenic strains, cocci *Staphylococcus aureus, Pseudomonas putida*, *Klebsiella pneumoniae* and *Escherichia coli*. The results showed that the compound exhibited significant activities in particular against *S. aureus*. Comparison with analogous reported Schiff bases allows us to conclude about the importance of the azo group in the structure of compound 2 for its antibacterial properties.

4. Materiel and methods:

4.1 Synthesis of Schiff base: 2

The N-(3-aminopropyl)imidazole (0.5 g, 4 mmol) was added to a methanol solution (30 ml) of 2-hydroxy-5-(-tolyldiazenyl)benzaldehyde (0.96 g, 4 mmol) prepared earlier [6]. The mixture was refluxed for 2 h and cooled to room temperature. The solvent was removed on a rotatory evaporator and the orange product was rinsed and recrystallized with a mixture of methanol and ether. The product was obtained as orange crystals [29].

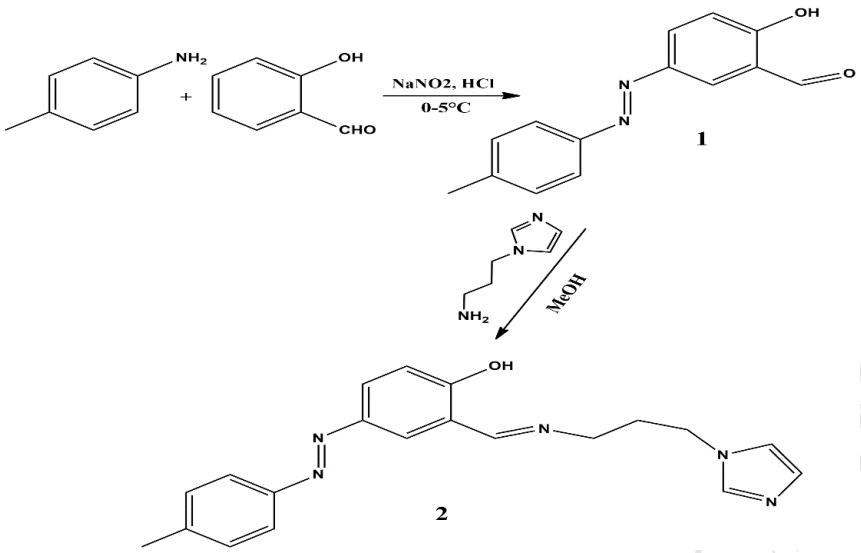

Scheme 1: Synthesis of Schiff base **2**

Yield 82%, m.p 95 °C. ^{1}H NMR (300MHz, [D_6]DMSO, 25°C, TMS) δ/ppm: 8.63 (s,1H), 7.99 (d,1H , J = 7.2), 7.88(dd, 1H, J = 6.6, J = 2.4), 7.71(d, 2H, J = 8.1), 7.65(s, 1H), 7.32(d, 2H, J = 8.1),7.19 (s, 1H), 6.90-7.00 (m, 2H), 4.04(t, 2H, J= 7.2), 3.55(t, 2H, J= 6.6), 2.34(s,3H), 2.13(qd, 2H, J=6.9). ^{13}C NMR (75 MHz, [D_6]DMSO, 25°C, TMS) δ/ppm: 21.49, 31.76, 44.34, 55.74, 117.95, 118.22, 118.73, 122.59, 126.93, 127.06, 129.77, 129.91, 137.12, 141.11, 145.46, 150.69, 163.80, 165.95. MALDI TOF MS calcd: m/z=347.17 Da. Found m/z= 348.4 $[M+1]^{+}$. HR-MS(M): for $C_{20}H_{21}N_5O$: 347.1746 found: 347.1745. Selected IR bands (cm^{-1}) 3105, 2943, 1634, 1580, 1485, 1445, 1377, 1283, 1229, 1107, 999, 959, 905, 851, 756, 689, 662. Anal. Calc. for $C_{20}H_{21}N_5O$: C, 69.14%; H, 6.09%; N, 20.16%. Found: C, 69.23%; H, 6.01%; N, 20.07%.

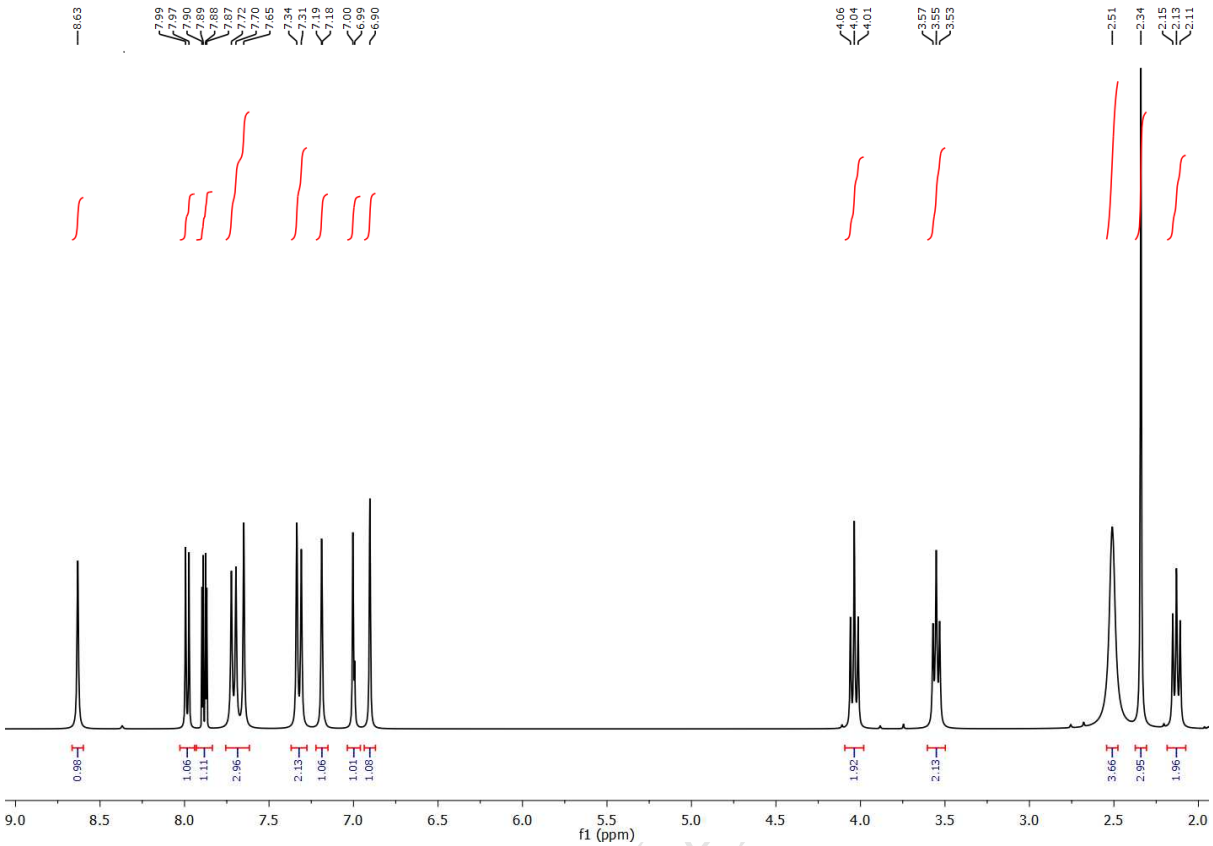

Figure 1: ^{1}H NMR spectrum of compound **2**

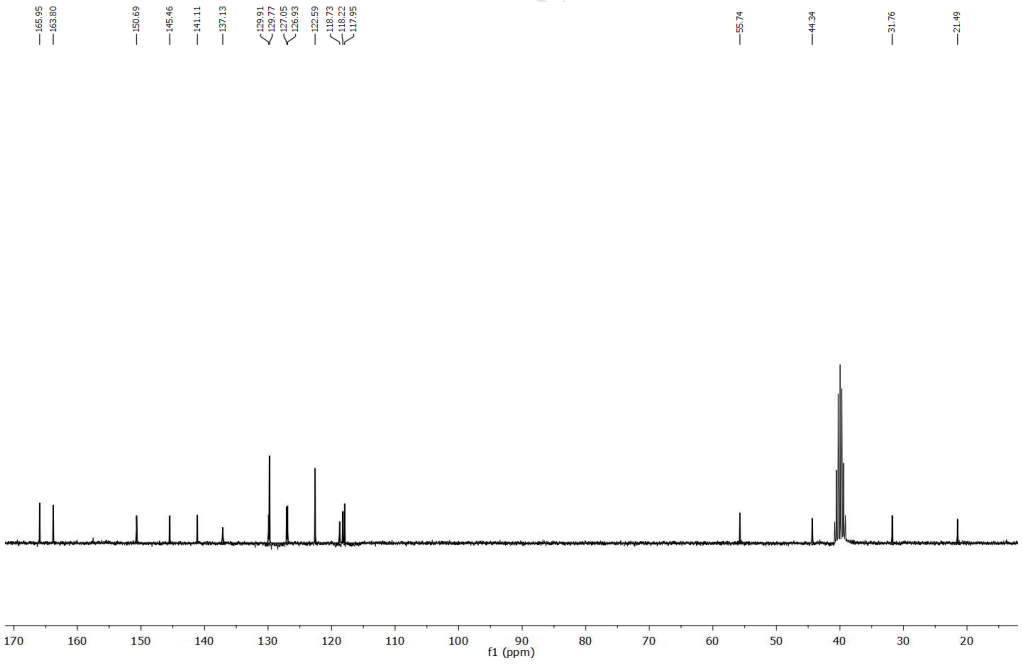

Figure 2: ^{13}C NMR spectrum of compound **2**

4.2 Single crystal X-ray diffraction:

A suitable single crystal was selected for X-ray diffraction analysis. Data of the compound was collected at room temperature with an Agilent SuperNova diffractometer using graphite monochromatized CuK_α radiation (λ = 1.54184 Å**),** equipped with a CCD area detector. The phase problem was solved by direct methods using SHELX97 programs [30]. The structural graphics were created using DIAMOND program. Experimental data collections details and the crystallographic features of (**2**) are reported in Table 1. The atomic coordinates and the basic geometrical data are reported in Tables 2 and 3.

4.3 DFT details:

The ground state geometry of schiff base **2** was optimized using DFT with Becke-3-Lee-Yang-Parr (B3LYP) exchange correlation functional with 6-31G(d) basis set for all atoms [31,32]. The calculation was carried out with Gaussian 09 software package without any symmetry constraint [33]. Then, the optimized geometry was used for energy calculations. Optical absorption spectra were simulated using the polarisable continuum model (PCM) with TD-DFT at B3LYP/6-31G(d), CAM-B3LYP/6-31G(d) and MPW1PW91/6-31G(d) levels , based on optimized ground state geometries. The PCM calculations have been performed in the chloroform solution.

4.4 Hirshfeld surfaces analysis:

Hirshfeld surfaces and fingerprint plots were generated for **2** based on the crystallographic information file (CIF) using CrystalExplorer [34,35]. Hirshfeld surfaces allow the visualization of intermolecular interactions. Colors and color intensities are related to the relative strength of the interaction and the short or long contacts.

4.5 Antibacterial activity:

The Schiff base **2** was tested for its antimicrobial activities against four bacterial strains, one Gram-positive cocci *Staphylococcus aureus* and three Gram-negative bacteria *Escherichia coli*, *Klebsiella pneumoniae* and *Pseudomonas putida* by the agar disc diffusion method using Muller Hinton agar. The strains were grown in Mueller-Hinton agar at 37 °C for 24 h and the suspension was prepared by matching a 0.5 McFarland standard. All the compounds were dissolved in dimethyl sulfoxide DMSO and tested by the procedure of measuring the inhibition zone, as described in literature [36,37]. The minimum inhibitory concentrations (MIC) of the schiff base **2** were also studied by liquid microdilutions method, using sterile 96-wells flat-shaped microtitre plates by serial dilution of the concentrations ranging from 145.16 to 7.42 $\mu g.mL^{-1}$. The commercially chloramphenicol was used as control drug. The analysis of both methods were made in three replicate for each compound.

References

[1] P. Przybylski, A. Huczynski, K. Pyta, B. Brzezinski, F. Bartl, Biological Properties of

Schiff Bases and Azo Derivatives of Phenols, Curr. Org. Chem. 13(2) (2009) 124–148.

[2] P.P. Dholakiya, M.N. Patel, Synthesis and Reactivity in Inorganic and Metal- Organic Chemistry Metal Complexes : Preparation , Magnetic , Spectral , and Biocidal Studies of Some Mixed Ligand Complexes with Schiff Bases Containing NO and NN Donor Atoms, (2010) 37–41. doi:10.1081/SIM-120030440.

[3] Z. Parsaee, K. Mohammadi, DFT calculations and antibacterial evaluation of new macrocyclic Schiff base compounds, J. Mol. Struct. 1137 (2017) 512–523. doi:10.1016/j.molstruc.2017.02.026.

[4] M. Kumar, K. Gupta, S. Chhibber, Synthesis , characterization and antibacterial studies of schiff based 1 , 2 , 3-triazole bridged silatranes, J. Organomet. Chem. 871 (2018) 21–27. doi:10.1016/j.jorganchem.2018.06.024.

[5] E. Gungor, S. Celen, D. Azaz, H. Kara, Two tridentate Schiff base ligands and their mononuclear cobalt (III) complexes: Synthesis, characterization, antibacterial and antifungal activities, Spectrochim. Acta - Part A Mol. Biomol. Spectrosc. 94 (2012) 216–221. doi:10.1016/j.saa.2012.03.034.

[6] S. Slassi, A. Fix-tailler, G. Larcher, A. Amine, A. El-ghayoury, Imidazole and Azo-Based Schiff Bases Ligands as Highly Active Antifungal and Antioxidant Components, Heteroatom Chem. 2019 (2019). DOI: 10.1155/2019/6862170.

[7] K.P. Rakesh, H.M. Manukumar, D.C. Gowda, Bioorganic & Medicinal Chemistry Letters Schiff ’ s bases of quinazolinone derivatives : Synthesis and SAR studies of a novel series of potential anti-inflammatory and antioxidants, Bioorg. Med. Chem. Lett. 25 (2015) 1072–1077. doi:10.1016/j.bmcl.2015.01.010.

[8] M. Nath, P. Kumar, A. Kumar, New di- and triorganotin (IV) complexes of tripodal Schiff base ligand containing three imidazole arms : Synthesis , structural characterization , anti-inflammatory activity and thermal studies, J. Organomet. Chem. 695 (2010) 1353–1362. doi:10.1016/j.jorganchem.2010.02.009.

[9] K. Zhang, P. Wang, L. Xuan, X. Fu, F. Jing, S. Li, Y. Liu, B. Chen, Bioorganic & Medicinal Chemistry Letters Synthesis and antitumor activities of novel hybrid molecules moiety, Bioorg. Med. Chem. Lett. 24 (2014) 5154–5156. doi:10.1016/j.bmcl.2014.09.086.

[10] M. Shebl, O.M.I. Adly, E.M. Abdelrhman, Binary and ternary copper (II) complexes of a new Schiff base ligand spectral , thermal , antimicrobial and antitumor studies, J. Mol. Struct. 1145 (2017) 329–338. doi:10.1016/j.molstruc.2017.05.064.

[11] Y. Wang, F. Xu, Y. Zhu, B. Song, D. Luo, G. Yu, Bioorganic & Medicinal Chemistry Letters Pyrazolo [3 , 4- d] pyrimidine derivatives containing a Schi ff base moiety as potential antiviral agents, Bioorg. Med. Chem. Lett. 28 (2018) 2979–2984. doi:10.1016/j.bmcl.2018.06.049.

[12] S. Murtaza, M. Shoaib, F. Kanwal, A. Abbas, S. Ashiq, S. Shamim, Synthesis and biological evaluation of schiff bases of 4-aminophenazone as an anti-inflammatory , analgesic and antipyretic agent, J. Saudi Chem. Soc. 21 (2017) S359–S372. doi:10.1016/j.jscs.2014.04.003.

[13] Y. Al-abed, L. Dubrovsky, B. Ruzsicska, Inhibition of HIV-1 Nuclear Import via Schiff Base Formation with Arylene Bis (methylketone) Compounds, 12 (2002) 3117–3119.

[14] W. Song, J. Cheng, D. Jiang, L. Guo, M. Cai, H. Yang, Spectrochimica Acta Part A : Molecular and Biomolecular Spectroscopy Synthesis , interaction with DNA and antiproliferative activities of two novel Cu (II) complexes with Schiff base of benzimidazole, SAA. 121 (2014) 70–76. doi:10.1016/j.saa.2013.09.142.

[15] B.N. Prasanna, K.N. Mohana, L. Mallesha, Synthesis and antiproliferative activity of some new fluorinated Schiff bases derived from 1 , 2 , 4-triazoles, J. Fluor. Chem. 156 (2013) 15–20. doi:10.1016/j.jfluchem.2013.08.008.

[16] T.G. Edwards, C. Fisher, Antiviral activity of pyrrole-imidazole polyamides against SV40 and BK polyomaviruses, Antiviral Res. 152 (2018) 68–75. doi:10.1016/j.antiviral.2018.02.012.

[17] D. Sharma, B. Narasimhan, P. Kumar, V. Judge, R. Narang, E. De Clercq, J. Balzarini, European Journal of Medicinal Chemistry Synthesis , antimicrobial and antiviral evaluation of substituted imidazole derivatives, Eur. J. Med. Chem. 44 (2009) 2347–2353. doi:10.1016/j.ejmech.2008.08.010.

[18] D. Schemeth, C. Kappacher, M. Rainer, R. Thalinger, G.K. Bonn, Talanta Comprehensive evaluation of imidazole-based polymers for the enrichment of selected non-steroidal anti-in fl ammatory drugs, Talanta. 153 (2016) 177–185. doi:10.1016/j.talanta.2016.03.015.

[19] I. Kr, New derivatives of imidazole as potential anticancer agents, 53 (1998) 342–345.

[20] A. Negi, J. Marin, S.M. Amrutkar, A.T. Baviskar, G. Joshi, S. Singh, U.C. Banerjee, R. Kumar, Bioorganic & Medicinal Chemistry Imine / amide – imidazole conjugates derived from 5-amino-4-cyano- N 1-substituted benzyl imidazole : Microwave-assisted synthesis and anticancer activity via selective topoisomerase-II- a inhibition, Bioorg. Med. Chem. 23 (2015) 5654–5661. doi:10.1016/j.bmc.2015.07.020.

[21] M. Taha, N. Hadiani, S. Imran, H. Rashwan, W. Jamil, S. Ali, S. Muhammad, F. Rahim, U. Salar, K. Mohammed, Bioorganic Chemistry Synthesis of 6-chloro-2-Aryl-1H-imidazo [4 , 5-b] pyridine derivatives : Antidiabetic , antioxidant , b -glucuronidase inhibiton and their molecular docking studies, Bioorg. Chem. 65 (2016) 48–56. doi:10.1016/j.bioorg.2016.01.007.

[22] K. Mahmood, W. Hashmi, H. Ismail, B. Mirza, B. Twamley, Z. Akhter, I. Rozas, R.J. Baker, Synthesis, DNA binding and antibacterial activity of metal(II) complexes of a benzimidazole Schiff base, Polyhedron. 157 (2019) 326–334. doi:10.1016/j.poly.2018.10.020.

[23] M. Salehi, A. Amoozadeh, A. Salamatmanesh, M. Kubicki, G. Dutkiewicz, S. Samiee, A. Khaleghian, Synthesis, characterization, crystal structures, computational studies, and antibacterial activities of two new Schiff bases derived from isophthalaldehyde, J. Mol. Struct. 1091 (2015) 81–87. doi:10.1016/j.molstruc.2015.02.060.

[24] A. Lapasam, V. Banothu, U. Addepally, M.R. Kollipara, Synthesis, structural and antimicrobial studies of half-sandwich ruthenium, rhodium and iridium complexes

containing nitrogen donor Schiff-base ligands, J. Mol. Struct. 1191 (2019) 314–322. doi:10.1016/j.molstruc.2019.04.116.

[25] M. Mesbah, T. Douadi, F. Sahli, S. Issaadi, S. Boukazoula, S. Chafaa, Synthesis, characterization, spectroscopic studies and antimicrobial activity of three new Schiff bases derived from Heterocyclic moiety, J. Mol. Struct. 1151 (2018) 41–48. doi:10.1016/j.molstruc.2017.08.098.

[26] S. Yousef Ebrahimipour, B. Machura, M. Mohamadi, M. Khaleghi, A novel cationic cobalt(III) Schiff base complex: Preparation, crystal structure, Hirshfeld surface analysis, antimicrobial activities and molecular docking, Microb. Pathog. 113 (2017) 160–167. doi:10.1016/j.micpath.2017.10.034.

[27] M. Kalanithi, M. Rajarajan & P. Tharmaraj, Synthesis, spectral, and biological studies of transition metal chelates of N-[1-(3-aminopropyl)imidazole]salicylaldimine, J. Coord. Chem. 64 (2011) 842-850. doi: 10.1080/00958972.2011.557432

[27] J. McGinley, M. McCann , K. Ni, T. Tallon, K. Kavanagh, M. Devereux, X. Ma, V. McKee, Imidazole Schiff base ligands: Synthesis, coordination complexes and biological activities, Polyhedron, 55 (2013) 169–178. http://dx.doi.org/10.1016/j.poly.2013.03.023

[29] S. Slassi, O. Stetsiuk, A. Amine, M. Aarjane, H. Zouihri, K. Yamni, data reports 4- [(E) - (4-methylphenyl) diazenyl] phenol, (2019). doi:10.1107/S2414314619000361.

[30] R. Herbst-irmer, G.M. Sheldrick, È.A. Chemie, D.- Go, Re ® nement of Twinned Structures with SHELXL 97, (1998). doi:10.1107/S0108768197018454.

[31] A.D. Becke, Density-functional thermochemistry . III . The role of exact exchange, 5648 (2001). doi:10.1063/1.464913.

[32] C. Lee, C. Hill, N. Carolina, into a functional of the electron density f f, 37 (1988).

[33] J.R.C. M. J. Frisch, G. W. Trucks, H. B. Schlegel, G. E. Scuseria, M. A. Robb, H.P. G. Scalmani, V. Barone, B. Mennucci, G. A. Petersson, H. Nakatsuji, M. Caricato, X. Li, K. Hratchian, A. F. Izmaylov, J. Bloino, G. Zheng, J. L. Sonnenberg, M. Hada, M. Ehara, T. Toyota, R. Fukuda, J. Hasegawa, M. Ishida, T. Nakajima, Y. Honda, O. Kitao, H. Nakai, K. Vreven, J. A. Montgomery, Jr., J. E. Peralta, F. Ogliaro, M. Bearpark, J. J. Heyd, E. Brothers, J.C. N. Kudin, V. N. Staroverov, R. Kobayashi, J. Normand, K. Raghavachari, A. Rendell, J.B. Burant, S. S. Iyengar, J. Tomasi, M. Cossi, N. Rega, J. M. Millam, M. Klene, J. E. Knox, A.J. Cross, V. Bakken, C. Adamo, J. Jaramillo, R. Gomperts, R. E. Stratmann, O. Yazyev, V.G.Z. Austin, R. Cammi, C. Pomelli, J. W. Ochterski, R. L. Martin, K. Morokuma, J.B. G. A. Voth, P. Salvador, J. J. Dannenberg, S. Dapprich, A. D. Daniels, O. Farkas, and D.J.F. Foresman, J. V. Ortiz, J. Cioslowski, Gaussian09, Revis. A.02, Gaussian, Inc., Wallingford CT. (2009).

[34] S. Partitioning, C. Density, Spatial Partitioning of Charge Density, 16 (1977) 198–201.

[35] D.P. Mackinnon, C.M. Lockwood, Multivariate Behavioral Confidence Limits for the Indirect Effect : Distribution of the Product and Resampling Methods, (2010) 37–41. doi:10.1207/s15327906mbr3901.

[36] A.L. Barry, M.B. Coyle, C. Thornsberry, E.H. Gerlach, R.W. Hawkinsons, B.E.T. Al, J.C. Microbiol, Methods of Measuring Zones of Inhibition with the Bauer- Kirby Disk Susceptibility Test, 10 (1979) 885–889.

[37] C.A. Alonso, C. Domínguez, J. Heras, E. Mata, V. Pascual, C. Torres, M. Zarazaga, Computer Methods and Programs in Biomedicine Antibiogramj : A tool for analysing images from disk diffusion tests, Comput. Methods Programs Biomed. 143 (2017) 159–169. doi:10.1016/j.cmpb.2017.03.010.

Table 1: Crystallographic data, details of data collection and structure refinement parameters for 2.

CCDC number	1889270
Chemical formula	$C_{20}H_{21}N_5O$
Mr	347.42
Crystal system, space group	Monoclinic, P2/n
Temperature (K)	293
a (Å)	12.2410 (4)
b (Å)	5.9386 (2)
c (Å)	25.2112 (9)
β (°)	90.317 (3)
V ($Å^3$)	1832.69 (11)
Z	4
Radiation type	Cu Kα
μ (mm-1)	0.65
Crystal size (mm)	0.35 × 0.22 × 0.13
No. of measured, independent and observed [I > 2σ(I)] reflections	5548, 3487, 3037
Rint	0.016
(sin θ/λ)max (Å-1)	0.622
R[F2 > 2σ(F2)], wR(F2), S	0.084, 0.245, 1.08
No. of reflections	3487
No. of parameters	236
Δρmax, Δρmin (e $Å^{-3}$)	1.02, -0.67

Table 2: Experimental and theoretical bond distances

Distance	Theoretical	Experimental
C13—C2	1.5097	1.501 (5)
C14—N3	1.2747	1.272 (4)
C14—C11	1.4711	1.457 (4)
C15—C16	1.535	1.500 (4)
C15—N3	1.4529	1.464 (3)
C16—C17	1.5341	1.520 (4)
C17—N4	1.4603	1.465 (3)
C18—N4	1.3687	1.347 (3)
C18—N6	1.3162	1.317 (3)
C19—C20	1.3732	1.354 (4)
C19—N4	1.3821	1.370 (3)
C20—N6	1.3765	1.367 (4)
C1—C2	1.4081	1.372 (5)
C1—C6	1.3868	1.427 (5)
C2—C3	1.3994	1.397 (5)
C3—C4	1.3936	1.333 (6)
C4—C5	1.3997	1.333 (6)
C5—C6	1.4071	1.426 (6)
C5—N1	1.4152	1.537 (5)
C7—C8	1.3969	1.381 (4)
C7—C11	1.4013	1.386 (4)
C8—C9	1.4061	1.399 (5)
C8—N2	1.4124	1.547 (5)
C9—C10	1.3844	1.385 (5)
C10—C12	1.4065	1.401 (4)
C11—C12	1.4164	1.417 (4)
O1—C12	1.3541	1.336 (3)
N1—N2	1.263	1.174 (4)

Table 3: Experimental and theoretical angles

Angle	Theoretical	Experimental
C18—N6—C20	104.8159	103.9 (2)
C2—C1—C6	119.3819	119.0 (4)
C1—C2—C3	118.1767	119.3 (4)
N3—C14—C11	125.7455	121.1 (3)
C1—C2—C13	120.4741	121.2 (4)
C3—C2—C13	121.3492	119.4 (4)
C4—C3—C2	120.8914	123.6 (4)
N3—C15—C16	109.9768	110.2 (2)
C3—C4—C5	120.4182	117.8 (4)
C4—C5—C6	119.2652	123.7 (4)
C15—C16—C17	113.7855	113.1 (2)
C4—C5—N1	115.7123	116.4 (4)
C6—C5—N1	125.0225	119.9 (4)
C5—C6—C1	119.7799	116.5 (4)
C8—C7—C11	122.796	121.6 (3)
N4—C17—C16	113.8787	111.5 (2)
C7—C8—C9	118.7645	119.0 (3)
C7—C8—N2	116.0647	111.1 (3)
C9—C8—N2	125.1708	129.8 (3)
C10—C9—C8	119.691	120.7 (3)
N6—C18—N4	112.6158	112.8 (2)
C9—C10—C12	121.3768	120.4 (3)
C20—C19—N4	105.6623	105.6 (2)
C7—C11—C12	117.5065	119.4 (3)
C19—C20—N6	110.7339	111.3 (2)
C7—C11—C14	117.313	119.5 (3)
C12—C11—C14	125.1804	121.1 (3)
O1—C12—C10	120.8141	119.6 (3)
C14—N3—C15	117.2776	119.3 (3)
O1—C12—C11	119.3208	121.5 (2)
C18—N4—C19	106.172	106.4 (2)
C10—C12—C11	119.8651	118.9 (3)
C18—N4—C17	126.9746	126.2 (2)
N2—N1—C5	114.8834	108.1 (3)
C19—N4—C17	126.8219	127.3 (2)
N1—N2—C8	114.7568	105.2 (3)

Highlights

- Synthesis and characterization of Schiff base based on imidazole is reported.

- The structure of Schiff base was confirmed by X-ray crystallography.

- The Schiff base was screened for its potential antibacterial.

- The structure of Schiff base was investigated using DFT and the nature of HOMO and LUMO, electronic absorption were theoretically studied.